Supernova 1987A:30 years later - Cosmic Rays and Nuclei from Supernovae and their aftermaths
Proceedings IAU Symposium No. 331, 2017
A. Marcowith, M. Renaud, G. Dubner, A. Ray & A. Bykov, eds.

doi:10.1017/S1743921317006342

Supernova remnants dynamics

Anne Decourchelle

Laboratoire AIM-Paris-Saclay, CEA/DSM/Irfu - CNRS - Universite Paris Diderot, CEA-Saclay, 91191 Gif sur Yvette, France,
email: anne.decourchelle@cea.fr

Abstract. Supernova remnants are the site of a number of physical processes (shock-heating, non-equilibrium ionization, hydrodynamic instabilities, particle acceleration, magnetic field amplification). Their related emission processes provide us with a large set of observational data. Supernova remnants result from the interaction of high-velocity material ejected by the supernova explosion with the medium surrounding the progenitor star. This interaction gives rise to a double-shock structure that lasts for hundreds of years, with a forward shock and a reverse shock compressing and heating to tens million of degrees the surrounding medium and the ejecta, respectively. It is mostly in this phase that young supernova remnants provide information on their explosion mechanism through spectro-imaging observations of the ejected nucleosynthesis products and their dynamics, notably in the X-ray domain. I will review these observations and their implications for our current understanding of the dynamics of supernova remnants. I will conclude on the prospects with future facilities.

Keywords. supernova remnants, kinematics and dynamics, hydrodynamics, cosmic rays, radiation mechanisms: nonthermal, radiation mechanisms: thermal

1. Introduction

The morphology of supernova remnants (SNRs) is driven by the initial explosion mechanism of the supernova and their subsequent interaction with the circumstellar environment/ambient interstellar medium. SNRs are traced by photons emitted through different radiation mechanisms arising from various physical processes and particle populations. As a consequence, observations of SNRs display various morphologies and features depending on their initial conditions, its subsequent evolution and their current evolutionary stage, as illustrated in X-rays in Fig. 1. They tell us a lot about the composition of the emitting plasma, its kinematics, local and global properties of the remnants, and they keep track of their evolution.

The main physical process is the interaction of high-velocity ejected material from the supernova (ejecta) with its surrounding medium, leading to the formation of a high Mach number shock propagating outwards into the ambient medium (hereafter, named forward shock). As introduced by McKee (1974), the deceleration of the ejected material by the ambient material gives rise to a shock propagating inwards into the ejecta (hereafter, named reverse shock). Both shocks are responsible for compressing and heating to high temperatures the ambient medium and ejecta, respectively. They are expected to produce X-ray bremsstrahlung and X-ray emission lines. The contribution of the shocked ejecta is strongly dominant compared to the shocked ambient medium in this phase for a number of factors (range of density and temperature, composition, non-equilibrium conditions,..). X-ray detections of the shocked ambient medium are indeed very limited in young SNRs (for example, Miceli *et al.* 2012). However, fast forward shocks have the ability to accelerate efficiently particles (Blandford & Eichler 1987). The electrons, accelerated to TeV energies

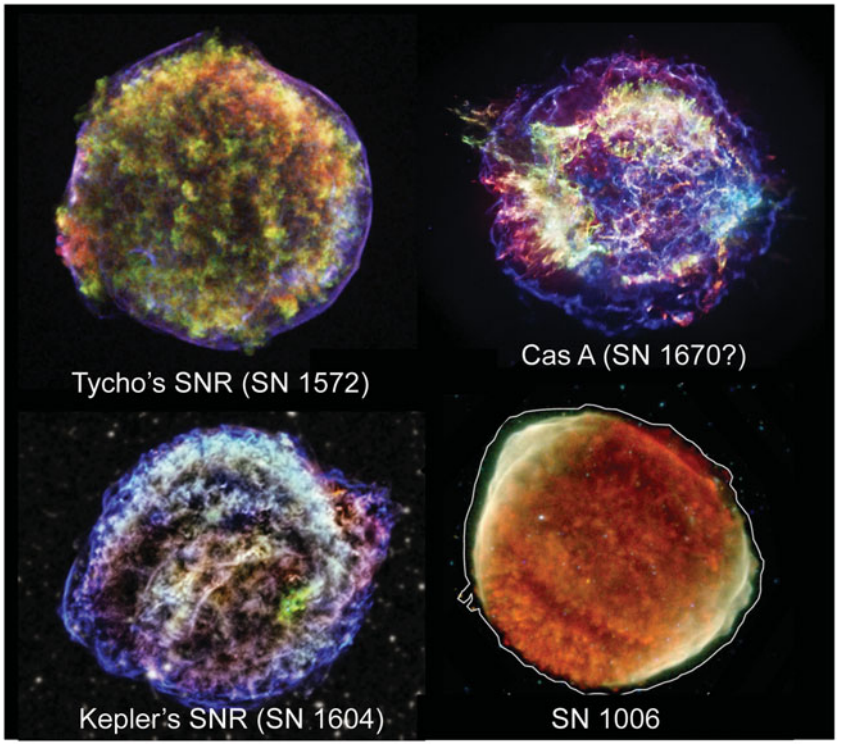

Figure 1. A gallery of young supernova remnants of different types and environments showing various X-ray morphologies observed with *Chandra* for Tycho's (Credit: NASA/CXC/Rutgers/J.Warren & J.Hughes *et al.*), Kepler's (Credit: NASA/CXC/NCSU/M.Burkey *et al.*; Optical: DSS) and Cas A's (NASA/CXC/SAO) SNRs and with *XMM-Newton* for SN1006 remnant (from Li *et al.* 2015). Note that the scale is different for each remnant.

at the forward shock, emit X-ray synchrotron emission that follows closely the forward shock rim. They can be observed as narrow filaments delineating the extension of young remnants, as seen in Fig. 1 for Tycho's, Kepler's, Cas A and SN1006 remnants. At the unstable interface between the ejecta and the ambient medium develop Rayleigh-Taylor instabilities that shape the observed fluffy X-ray ejecta emission. The Rayleigh-Taylor fingers emission from the ejecta comes relatively close to the forward shock. In between, the shocked ambient medium is invisible.

2. Hydrodynamics of young supernova remnants

In this section, I will review the hydrodynamic profile of the interaction region, bounded by both forward and reverse shocks, and which depends on the initial density profile of both the ejected material from the supernova and the ambient medium.

Chevalier (1982) has shown that in the case of expanding ejecta with a power-law density profile interacting with a stationary power-law density profile ambient medium, self-similar solutions for the structure of the interaction region can be obtained. They depend on the power law index of both density profiles. The observations of SN 1987A gave for the first time the opportunity to quantitatively challenge existing theories of core collapse supernovae and to provide constraints to the models. From the light curve constraints, Arnett (1988) derived the evolution of the ejecta density profile from core

https://doi.org/10.1017/S1743921317006342 Published online by Cambridge University Press

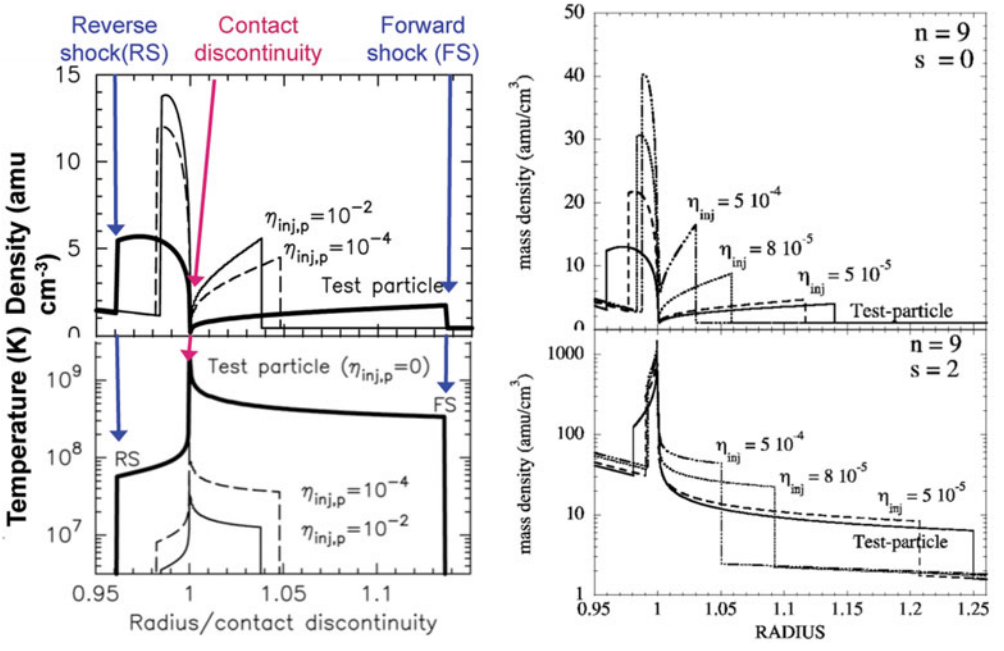

Figure 2. Left : Density and temperature structure of the interaction region for different values of the fraction of accelerated ions (from Decourchelle, Ballet, & Ellison 2000). Right : Density structure with (bottom) and without stellar wind (top) for different values of the fraction of accelerated ions.

collapse to its further evolution up to 1.85 days (see Fig. 4 in Arnett 1988). After core collapse, the shock took about 50 minutes to propagate from the core to the stellar surface. The ejecta density structure has then a steep dependence with radius in coherence with the surface layers of an hydrostatic object. As a result of the non-homologous expansion, the shock propagating through this structure accelerates and produces a power-law density profile, which is effective about 10 hours after the core collapse of SN1987A. In the phase where the self-similar solutions of Chevalier (1982) describe the evolution of the remnant, the behavior depends upon a combination of kinetic energy of the explosion per unit mass ejected. Once the reverse shock has propagated out of the power-law density profile into the inner flatter core of the ejecta, the Chevalier self-similar solutions do not apply anymore. It is by following the further evolution of the remnant that both parameters could be separately determined.

The density structure of the interaction region has also been investigated in the case of an exponential density profile in the ejecta, that approximates a set of Type Ia explosion models (Dwarkadas & Chevalier 1998). Compared to power-law profiles, one of the main results is a much flatter temperature profile in the ejecta, not favored by X-ray observations of young type Ia remnant like Tycho's SNR that indicate significant temperature variations in the ejecta.

These previous hydrodynamic models were not considering the back-reaction of particle acceleration at the shocks. However, shocks in SNRs are thought to provide a significant fraction of cosmic rays up to energies close to the knee at about 3 10^{15} eV. If a significant fraction of ions is accelerated at the shocks, it modifies the compressibility of the shocked gas and the shock properties with an overall compression ratio larger than 4 (Axford 1981). The overall interaction structure is modified as shown by Chevalier (1983), who investigated the effects of cosmic-ray pressure on the dynamics of self-similar

https://doi.org/10.1017/S1743921317006342 Published online by Cambridge University Press

solutions with a prescribed back-reaction of the accelerated particles. Decourchelle, Ballet & Ellison (2000) coupled these solutions to a model of ion diffusive acceleration at the shock (Berezhko & Ellison 1999) to investigate and quantify the impact on the interaction structure as a function of the fraction $\eta_{\rm inj,p}$ of protons injected into the acceleration process. When the injection $\eta_{\rm inj,p}$ is large, the compression ratio is larger than 4, the post-shock temperature is decreased and the shocked region shrinks very significantly, compared to test-particle conditions. As a result, the shock gets closer to the contact discontinuity (see Fig. 2). This is what is observed in young remnants like Tycho's and Kepler's SNR (see Fig. 1), where the forward shock is close to the contact discontinuity. This proves that ion acceleration is very efficient at the forward shock in these remnants. The distance between the forward shock and the contact discontinuity can thus provide an estimate of the efficiency of ion acceleration at the shock (see for Tycho's SNR, Warren *et al.* 2005).

The structure of the interaction region is also dependent on the nature of the ambient medium (mass density $\rho \propto r^{-s}$), notably if there is a circumstellar wind ($s = 2$), or a uniform interstellar medium ($s = 0$). A comparison between these two cases is shown in Fig. 2 (right panel) showing important differences in the structure in terms of extent and density profile of the shocked regions. The shocked ejecta are much compressed in presence of a stellar wind and displays a stronger density gradient, while the shocked ejecta are more extended than in the case of a uniform medium.

The above models are one dimensionals. There are however a few reasons why the evolution of young SNRs will not follow spherical symmetry. The first physical one is the development of Rayleigh-Taylor instabilities leading to large distortions of the shocked ejecta close to the contact discontinuity (Chevalier, Blondin & Emmering 1992), which distort in response the reverse shock and let unaffected the forward shock. Including efficient prescribed back-reaction from accelerated particle leads to possible distortion of the forward shock as well, as a result of its proximity to the contact discontinuity (Blondin & Ellison 2001). Three-dimensional simulations of young SNRs including nonlinear particle acceleration have been developed by Ferrand *et al.* (2010) coupling a semi-analytical kinetic model of shock acceleration (Blasi 2004) with a 3D hydrodynamic code *RAMSES* (Teyssier 2002). Coupling 3D calculations of the out-of-equilibrium thermal X-ray emission, as well as the broad range non-thermal emission, enables synthetic emission maps of young SNRs to be confronted to the characteristic features of the observations (Ferrand, Decourchelle & Safi-Harb 2012, 2014).

3. Morphological and spectral properties of a sample of SNRs

The evolution, morphology, and spectral properties of young SNRs retain information on the physics of the explosion and on its environment. The quantities of synthesized elements depend on the SN type and the physics of the explosion. Their distribution, as well as the structure of the various physical quantities in the remnant, are markers of the initial event and its initial and subsequent conditions. The aim is to use this information to set constraints on the physics of supernovae.

For thermonuclear supernovae (SN Ia), one of the main issues concerns the nature of the companion in the binary system and the scenario leading to the explosion, either through a single degenerate system with a normal star as a companion, or through a double degenerate scenario with a white dwarf as a companion. A central question concerns the ignition of the burning and the propagation of the burning front. From the ratio between intermediate elements and iron in SN Ia, constraints could be set on the

https://doi.org/10.1017/S1743921317006342 Published online by Cambridge University Press

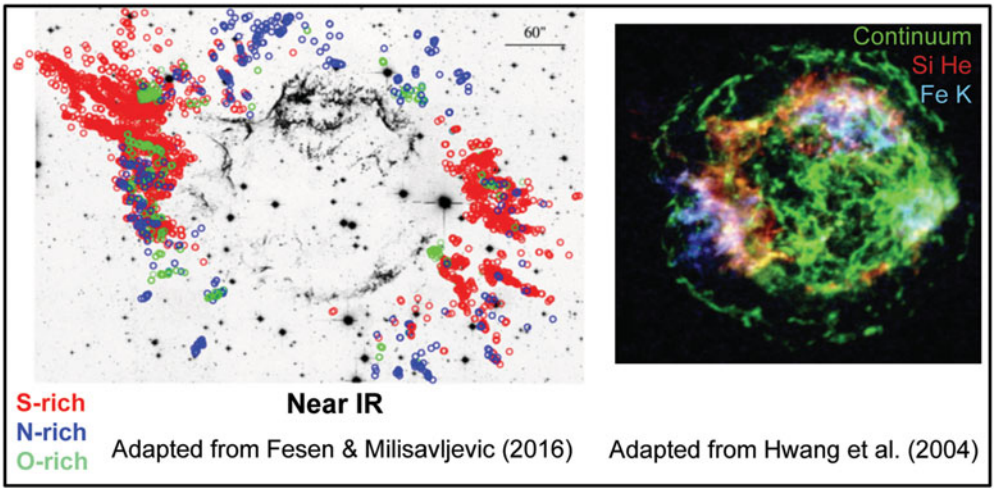

Figure 3. Cas A: Near IR image showing S-rich, N-rich et O-rich ejecta knots (left) and X-ray Chandra composite image (right, Credit: NASA/CXC/GSFC/U.Hwang *et al.*)

accretion rate from the companion star, and on the physics of propagating flame fronts (slow to fast deflagration, transition to detonation).

For core collapse supernovae, the issues deal with in particular the explosion mechanism (and related progenitors) and the value of the mass-cut to form the compact object. Elements lighter than silicon, that are produced mainly during hydrostatic evolution and spread away during the explosion, depend on the progenitor. The intermediate elements, enhanced through explosive oxygen burning, inform about the explosion energy and amount of matter accreted onto the core before the explosion. The iron-group nuclei provide detailed information on the explosion and mass-cut.

The morphology of a sample of 24 SNRs in the Milky Way and Large Magellanic Cloud has been investigated by Lopez *et al.* (2011), using statistical tools to analyze Chandra X-ray images. As a result, the authors found a clear trend in the morphology: type Ia SNRs are more symmetrical than core collapse SNRs. A systematic study of the energy of the iron K line in a sample of 23 SNRs observed with the X-ray satellite *Suzaku* was undertaken by Yamaguchi *et al.* (2014). It revealed a clear separation between type Ia SNRs with a lower centroid energy (low ionisation state) and core collapse SNRs with a higher centroid energy and higher Fe ionization state. This is a signature of different circumstellar media in both types of SNRs: Type Ia are compatible with an unmodified uniform ambient medium while core collapse supernovae explode in a circumstellar medium shaped by the progenitor wind. The overall X-ray spectra can in addition set constraints to the plausible theoretical models of both type Ia (Yamauchi *et al.* 2014) and core collapse supernovae (Patnaude *et al.* 2015).

4. A close-up view of Cassiopeia A and Tycho

Cassiopeia A (Cas A) is the remnant of a young core collapse supernova, on which has focused a large number of observations in the full electromagnetic range. Cas A evolves in a circumstellar medium resulting from the mass loss of its progenitor. As a result, the forward shock is in average significantly ahead of the contact discontinuity and of ejecta material, as expected from the hydrodynamical evolution of a remnant in

https://doi.org/10.1017/S1743921317006342 Published online by Cambridge University Press

a stellar wind (see Fig. 2, bottom right panel, case $s = 2$). However, X-ray observations with *Chandra* (Hughes *et al.* 2000) show a highly non-uniform distribution of elements in the shocked ejecta, reaching in some places the blast wave. They reveal a spatial inversion of a significant portion of the supernova core with the iron emission ahead of the silicon emission. The million second observation of Cas A with *Chandra* clearly reveals the bipolar structure, already observed in the optical (Fesen 2001 et references therein), of the Si-rich ejecta in the northeast and southwest directions (Hwang *et al.* 2004). Its origin has been debated with regard to the explosion mechanism of core collapse supernovae, but with insufficient energy associated with the jets to drive the explosion (Laming *et al.* 2006). Bulk X-ray Doppler velocities were derived from *XMM-Newton* (Willingale *et al.* 2002) and *Chandra* (Hwang *et al.* 2001) observations with a line-of-sight velocity scale around 2000-3000 km/s. They confirm a highly asymmetric explosion in an inhomogeneous environment with in particular two large clumps of iron expanding faster than silicon and sulphur. These measurements provide a deep insight into the explosion mechanism and expansion of the ejecta and are complementary to velocity patterns in the optical for much denser ejecta. A comparison of X-ray and optical emission, performed by Patnaude & Fesen (2014), shows the absence of significant large scale correlation but points to a number of correlated small scale features, which can be explained if the ejecta are highly inhomogeneous and display a range of densities. In the optical and near infrared, there are a very large number of detected knots spanning a large range of velocities and elements. The highest velocity metal-rich knots are located outside the outer blast wave of Cas A. They are interacting with the local unshocked circumstellar medium and gradually get disrupted. Deep HST WFC3/IR images of Cas A detected roughly 3400 outlying sulfur emitting knots with estimated velocities close to 15 000 km/s (Fesen & Milisavlevic 2016). The observed northeast and southwest jet structures are estimated to contain about 10% of the canonical 10^{51} ergs kinetic energy of the supernova. Their composition and velocities differ from any observed areas of Cas A. These findings are consistent with the dynamical scenario put forward by Burrows (2005), where jets from the proto-neutron star, produced after the neutrino-driven supernova explosion, pushed the turbulent inhomogeneous supernova ejecta. Further information from the innermost ejecta arose recently from NuSTAR observations of Cas A, and of its ^{44}Ti line emission, resulting from radioactive decays (Grefenstette *et al.* 2017).

Tycho's SNR is the remnant of a thermonuclear type Ia supernova, whose explosion was observed by the Danish astronomer Tycho Brahe in 1572. It is considered as a prototype of type Ia remnant. Its morphology is globally regular, but displays small scale inhomogeneities and large scale features. Constraints on the explosion mechanism came through its global X-ray spectrum (Decourchelle *et al.* 2001), whose spectral features are best explained by a delayed detonation models (Badenes *et al.* 2006). A fantastic observation was that of the optical light echo of the supernova event scattering on ambient interstellar clouds, whose spectrum was shown to be perfectly consistent with spectra of extragalactic standard type Ia supernovae (Krause *et al.* 2008). A thorough investigation of the spatial distribution of the shocked elements using *XMM-Newton* has put into evidence a radial stratification of the ejecta composition (see Fig. 4, left panel) with Fe located inner to the Ca and Si, as well as anisotropies in the distribution of Ca-rich and Fe-rich ejecta (Miceli *et al.* 2015). The region with high iron equivalent width shows indications of Ti line emission, in addition to Cr. The iron-peak nuclei seem to be spatially correlated in the ejecta, in agreement with the expectations from type Ia models. However, observations with *Suzaku* revealed that the outer southeast iron knot exhibits no emission from Cr, Mn or Ni, pointing at a peak temperature of roughly 5.4×10^9 K and a neutron excess of less than 2×10^{-3} (Yamaguchi *et al.* 2017). This

https://doi.org/10.1017/S1743921317006342 Published online by Cambridge University Press

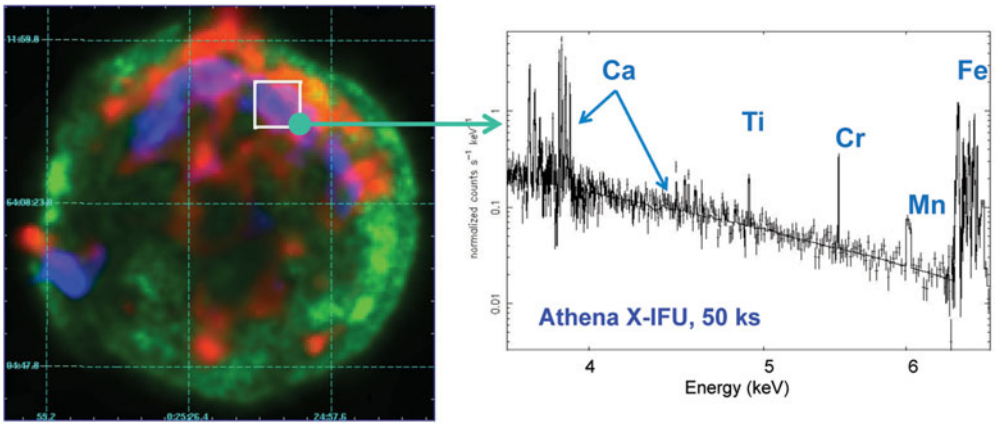

Figure 4. Left: *XMM-Newton* EPIC color-composite image of Tycho's SNR in the 4.4-6.1 keV energy band (green) and of the Ca (red) and Iron (blue) equivalent width (see Miceli *et al.* 2015). Right: *Athena* X-IFU 50 ks simulations of the spectrum of a region of 1 arcmin^2 region in Tycho's SNR (Courtesy of Marco Miceli).

rules out an origin of this knot in the deep, dense core of a Chandrasekhar-mass white dwarf and favors either incomplete Si burning or an α-rich freeze-out regime, probably close to the boundary of the remnant.

X-ray observations, in complement notably to optical and infrared observations, are keys to investigate the composition, kinematics and properties of the ejecta in young SNRs. X-rays give specifically access to the hot plasma of the shocked ejecta and provide diagnostics on the emitting conditions (ionization state of the elements, temperatures, densities). The progress in the field of young SNRs has been considerable since the launch of *Chandra* and *XMM-Newton* X-ray observatories, thanks to their capability of performing spatially resolved spectroscopy. However, to progress in the understanding of the explosion mechanism at play in supernovae, a key observational requirement is to improve on the spectral resolution of current X-ray spectro-imagers, which hampers our scientific investigation of the 3D structure and properties of the shocked ejecta. This is what will be possible with the ESA *Athena* X-ray observatory.

5. A new X-ray mission for spatially-resolved high-resolution spectroscopy : Athena

Athena is the ESA L2 mission, selected in June 2014, and dedicated to the hot and energetic Universe. The launch is planned for 2028 with an Ariane 6 rocket on an L2 orbit. It consists of a telescope, based on Silicon Pore Optics, of 2 m^2 at 1 keV and 5 arcsec HEW for a focal length of 12 m (Willingale *et al.* 2013) and of two instruments:
- the X-IFU (X-ray Integral Field Unit) designed to provide a spectral resolution of 2.5 eV, a field of view of 5 arcmin (Barret *et al.* 2013).
- the WFI (Wide Field Imager), designed to provide an energy resolution of 125 eV and a large field of view of 40 arcmin, with a high countrate capability (Rau *et al.* 2013).

The expected impact of Athena in the study and understanding of SNRs is fantastic, covering a number of key issues in the field (Decourchelle *et al.* 2013).

Athena will be in particular revolutionary for investigating young SNRs. The X-IFU instrument, with its high energy resolution, combined with a good spatial resolution, and

https://doi.org/10.1017/S1743921317006342 Published online by Cambridge University Press

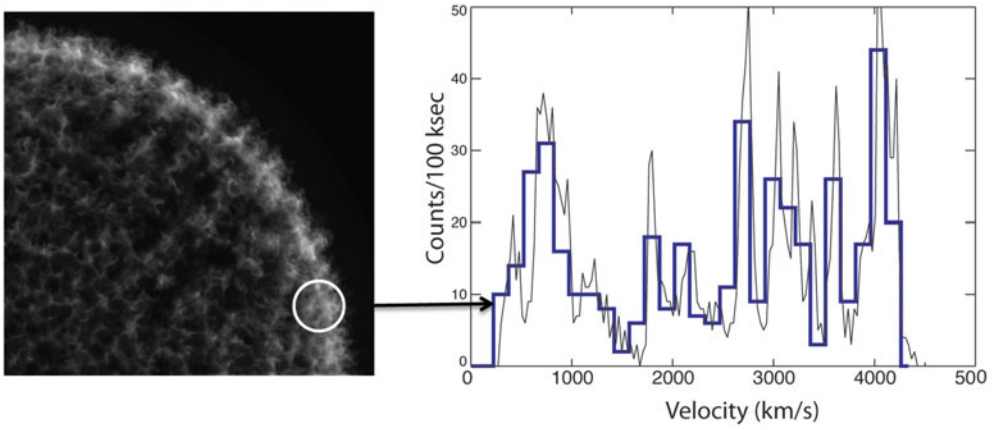

Figure 5. Left: Numerical 3D simulations of thermal X-ray emission in Tycho-like SNR (Ferrand, Decourchelle, Safi-Harb 2014). Right: Expected *Athena* X-IFU line-of-sight velocity structure in the silicon K line of a region in the simulated ejecta (circle in left panel). In solid line, the profile derived from hydrodynamical simulations, in bold line *Athena* X-IFU simulations (Courtesy: A. Decourchelle, G. Ferrand & R. Smith).

large effective area, will provide the first detailed 3D mapping of the hot ejected material by deciphering the various ejecta components in the line of sight and will give access to emission lines from rare elements, like Titanium, Chromium and Manganese. Figure 4 (right panel) shows the X-IFU expected spectrum from a iron-rich region in Tycho's SNR. The faint Ti K line is detected at 6 sigma in a region of 1 arcmin^2.

Each observed region of the remnant includes a range of velocities in the line of sight that depends, as presented previously, upon the hydrodynamic structure of the interaction region, as well as local instabilities and initial stratification/inhomogeneities of the supernova material. The objective is to measure the velocity of the ejecta structures in the line of sight as a function of position in the remnant, along with the elemental abundances, temperatures, and ionization states. This will allow us to determine the geometry, the structure and properties of the ejecta, offering an insider view into the supernova explosion, revealing the underlying explosion mechanism, the initial conditions in the progenitor, as well as structures in the circumstellar and interstellar media. Figure 5 illustrates the ability of *Athena* X-IFU to recover the line-of-sight velocity structure of the bright Si K line in the ejecta.

6. Conclusion

Multi-wavelength observations of young galactic SNRs have provided a wealth of information on the nucleosynthesis yields, the dynamics of the ejecta and its asymmetries/inhomogeneities, the wide range of conditions in the ejecta from dense optical knots to diffuse X-ray plasma and the properties of the shocks. As a result, the observational constraints are tightened on the physics of the explosion and the properties of the progenitor. However, we lack a detailed 3D mapping of the distribution and conditions of the different elements in the hot ejecta that encompasses a large fraction of the remnant, and that is intimately linked to the supernova explosion mechanism and to the progenitor properties. The need is to perform spectroscopic diagnostics at the relevant spatial scales, including rare elements, to yield bulk and turbulent velocities, temperatures, ionization states and abundances of the various components of the shocked ejecta. *Athena* L2 ESA mission, to be launched in 2028, is awaited to fulfill these objectives.

https://doi.org/10.1017/S1743921317006342 Published online by Cambridge University Press

References

Arnett, W. D. 1988, *ApJ*, 331, 377

Axford, W. I. 1981, in: G. Setti, G. Spada, & A. W. Wolfendale (eds.), *Origin of Cosmic Rays*, Proc. IAU Symposium No. 94 (Dordrecht: Reidel), p. 339

Badenes, C., Borkowski, K. J., Hughes, J. P., Hwang, U., & Bravo, E. 2006, *ApJ*, 645, 1373

Barret, D., den Herder, J.-W., Piro, L., Ravera, L., *et al.* 2013, *Supporting paper for the science theme "The Hot and Energetic Universe" to be implemented by the Athena+ X-ray observatory*, astro-ph/arXiv:1308.6784

Berezhko, E. G. & Ellison, D. C. 1999, *ApJ*, 526, 385

Blandford, R. D. & Eichler, D. 1987, *Phys. Report*, 154, 1

Blasi, P. 2004, *Astropart. Phys*, 21, 45

Blondin, J. M. & Ellison, D. C. 2001, *ApJ*, 560, 244

Burrows, J. M., 2005, in: M. Turatto, S. Benetti, L. Zampieri, & W. Shea (eds) *1604-2004: Supernovae as Cosmological Lighthouses*, Proc. ASP Conf. Ser. No. 342 (San Francisco: Astronomy Society of the Pacific), p184

Chevalier, R. A. 1982, *ApJ*, 258, 790

Chevalier, R. A. 1983, *ApJ*, 258, 790

Chevalier, R. A., Blondin, J. M., & Emmering, R. T. 1992, *ApJ*, 392, 118

Decourchelle, A., Ballet, J., & Ellison, D. C. 2000, *ApJ*, 365, L218

Decourchelle, A., *et al.* 2001, *ApJ*, 543, L57

Decourchelle, A., Costantini, E., Badenes, C., Ballet, J., & Bamba, A. *et al.* 2013, *Supporting paper for the science theme "The Hot and Energetic Universe" to be implemented by the Athena+ X-ray observatory*, astro-ph/arXiv:1306.2335

Dwarkadas, V. V. & Chevalier, R. A. 1998, *ApJ*, 497, 807

Ferrand, J., Decourchelle, A., Ballet, J., Teyssier, R., & Frachetti, F. 2010, *A&A*, 509, L10

Ferrand, J., Decourchelle, A., & Safi-Harb, S. 2012, *A&A*, 760, 34

Ferrand, J., Decourchelle, A., & Safi-Harb, S. 2014, *A&A*, 789, 49

Fesen, R. A. 2001, *ApJS*, 133, 161

Fesen, R. A. & Milisavljevic, D. 2016, *ApJ*, 818, 17

Grefenstette,J. P. *et al.* 2017, *ApJ*, 834, 19

Hughes,J. P., Rakowski,C. E., Burrows, D. N. & Slane, P. O. 2000, *ApJ*, 528, L109

Hwang, U., Szymkowiak, A. E., Petre, R., & Holt, S. S. 2001, *ApJ*, 560, L179

Hwang, U., *et al.* 2004, *ApJ*, 615, L117

Li, J.-T., Decourchelle A., Miceli, M., Vink, J., & Bocchino, F. 2015, *MNRAS*, 453, 3953

Krause, O., *et al.* 2008, *Nature*, 456, 617

Laming, J. M., Hwang, U., Radics, B., Lekli, G., & Takacs, E. 2006, *ApJ*, 644, L260

Lopez, L. A., Ramirez-Ruiz, E., Huppenkothen, D., Badenes, C., & Pooley, D. A. 2011, *ApJ*, 732, 114

Miceli, M., Bocchino, F., Decourchelle, A., Maurin, G., Vink, J., *et al.* 2012, *A&A*, 546, A66

Miceli, M., Sciortino, S., Troja, E., & Orlando, S., 2015, *ApJ*, 805, 120

McKee, C. F. 1974, *ApJ*, 188, 335

Patnaude, D. J. & Fesen, R. A. 2014, *ApJ*, 789, 138

Patnaude, D. J. *et al.* 2015, *ApJ*, 803, 101

Rau, A., Meidinger, N., Nandra, K., Porro, M., Barret, D., et al. 2013, *Supporting paper for the science theme "The Hot and Energetic Universe" to be implemented by the Athena+ X-ray observatory*, astro-ph/arXiv:1308.6785

Warren, J. S., Hughes, J. P., Badenes, C., Ghavamian, P., McKee, C. F. *et al.* 2005, *ApJ*, 634, 376

Willingale, R., Bleeker, J. A. M., van der Heyden, K. J., Kaastra, J. S., & Vink, J. 2002, *A&A*, 381, 1039

Willingale, R., Pareschi, G., Christensen, F., & den Herder, J.-W. 2013, *Supporting paper for the science theme "The Hot and Energetic Universe" to be implemented by the Athena+ X-ray observatory*, astro-ph/arXiv:1307.1709

Yamaguchi, H., Badenes, C., Petre, R., Nakano, T., Castro, D. *et al.* 2014, *ApJ*, 785, L27

Yamaguchi, H., Hughes, J. P., Badenes, C., Bravo, E., Seitenzahl, I. V., *et al.* 2017, *ApJ*, 834, 124

https://doi.org/10.1017/S1743921317006342 Published online by Cambridge University Press